ISSN 1674-1056
http://cpb.iphy.ac.cn
http://iopscience.iop.org/cpb
中国物理 B
Chinese Physics
中国物理 Chinese Physics B

Magnetization-direction-dependent inverse spin Hall effect observed in IrMn/NiFe/Cu/YIG multilayer structure

Runrun Hao(郝润润), Ruxue Zang(臧如雪), Tie Zhou(周铁), Shishou Kang(康仕寿), Shishen Yan(颜世申), Guolei Liu(刘国磊), Guangbing Han(韩广兵), Shuyun Yu(于淑云), Liangmo Mei(梅良模)

Citation: Chin. Phys. B . 2019, 28(3): 037202. **doi:** 10.1088/1674-1056/28/3/037202
Journal homepage: http://cpb.iphy.ac.cn; http://iopscience.iop.org/cpb

What follows is a list of articles you may be interested in

Effects of the band-filling and Fe/Mo disorder on physical properties of Ca_2FeMoO_6

Jin-Feng Wang(王金凤), Zhao-Tong Zhuang(庄照通), Shuai-Shuai Liu(刘帅帅), Qian-Qian Gao(高迁迁)

Chin. Phys. B . 2018, 27(12): 127201. **doi:** 10.1088/1674-1056/27/12/127201

Spin-independent transparency of pure spin current at normal/ferromagnetic metal interface

Runrun Hao(郝润润), Hai Zhong(钟海), Yun Kang(康韵), Yufei Tian(田雨霏), Shishen Yan(颜世申), Guolei Liu(刘国磊), Guangbing Han(韩广兵), Shuyun Yu(于淑云), Liangmo Mei(梅良模), Shishou Kang(康仕寿)

Chin. Phys. B . 2018, 27(3): 037202. **doi:** 10.1088/1674-1056/27/3/037202

The origin of spin current in YIG/nonmagnetic metal multilayers at ferromagnetic resonance

Yun Kang(康韵), Hai Zhong(钟海), Runrun Hao(郝润润), Shujun Hu(胡树军), Shishou Kang(康仕寿), Guolei Liu(刘国磊), Yin Zhang(张引), Xiangrong Wang(王向荣), Shishen Yan(颜世申), Yong Wu(吴勇), Shuyun Yu(于淑云), Guangbing Han(韩广兵), Yong Jiang(姜勇), Liangmo Mei(梅良模)

Chin. Phys. B . 2017, 26(4): 047202. **doi:** 10.1088/1674-1056/26/4/047202

Spin pumping through magnetic impurity effect

Deng Wei-Yin, Sheng Li, Xing Ding-Yu

Chin. Phys. B . 2015, 24(8): 087202. **doi:** 10.1088/1674-1056/24/8/087202

Spin transport in a Zigzag normal/ferromagnetic graphene junction

Shi Hao-Sheng, Vahram L. Grigoryan

Chin. Phys. B . 2015, 24(5): 057202. **doi:** 10.1088/1674-1056/24/5/057202

Magnetization-direction-dependent inverse spin Hall effect observed in IrMn/NiFe/Cu/YIG multilayer structure*

Runrun Hao(郝润润), Ruxue Zang(臧如雪), Tie Zhou(周铁), Shishou Kang(康仕寿)†, Shishen Yan(颜世申), Guolei Liu(刘国磊), Guangbing Han(韩广兵), Shuyun Yu(于淑云), and Liangmo Mei(梅良模)

School of Physics and State Key Laboratory of Crystal Materials, Shandong University, Jinan 250100, *China*

(Received 12 November 2018; revised manuscript received 4 January 2019; published online 26 February 2019)

The magnetization-direction-dependent inverse spin Hall effect (ISHE) has been observed in NiFe film during spin Seebeck measurement in IrMn/NiFe/Cu/yttrium iron garnet (YIG) multilayer structure, where the YIG and NiFe layers act as the spin injector and spin current detector, respectively. By using the NiFe/IrMn exchange bias structure, the magnetization direction of YIG ($M_{\rm YIG}$) can be rotated with respect to that of NiFe ($M_{\rm NiFe}$) with a small magnetic field, thus allowing us to observe the magnetization-direction-dependent inverse spin Hall effect voltage in NiFe layer. Compared with the situation that polarization direction of spin current ($\sigma_{\rm s}$) is perpendicular to $M_{\rm NiFe}$, the spin Seebeck voltage is about 30% larger than that when $\sigma_{\rm s}$ and $M_{\rm NiFe}$ are parallel to each other. This phenomenon may originate from either or both of stronger interface or bulk scattering to spin current when $\sigma_{\rm s}$ and $M_{\rm NiFe}$ are perpendicular to each other. Our work provides a way to control the voltage induced by ISHE in ferromagnets.

Keywords: spin current, magnetic insulator, inverse Hall effect

PACS: 72.25.Mk, 72.25.Rb, 72.25.–b, 75.70.Cn **DOI:** 10.1088/1674-1056/28/3/037202

1. Introduction

Generation and manipulation of pure spin current, which have attracted a great deal of attention, play important roles in spintronic devices.[1,2] Spin pumping,[3–6] spin Hall effect (SHE),[7,8] and spin Seebeck effect (SSE) provide several means to generate pure spin current.[8–10] Particularly, SSE in ferromagnetic insulators is an attractive one, which generates the spin current by a thermal gradient applied across a ferromagnetic insulator without any charge flow. When a spin current is injected into an adjacent material with large spin–orbit coupling, a transverse charge current will be induced in the direction perpendicular to both its polarization direction and flow direction via inverse spin Hall effect (ISHE).[4,11] The non-magnetic 5d metals, such as Pt, Ta, and W, are the common materials for spin current detectors.[12] In addition, comparatively large ISHE signals in ferromagnetic metals (FMs) have also been observed.[13–18] However, the situation in FM is more complicated since the conducting electrons are polarized, which means that the numbers of electrons with opposite spin are not equal. The scattering strength on spin electrons in FM depends on the relative orientation of the spin-polarized charge current and FM magnetization ($M_{\rm FM}$), which has been observed in the FM/normal mental/FM (or FM/insulator/FM) spin valve structure.[19–22] Very recently, in a ferroic collinear multilayer spin valve, the detection of the spin current emitted by ferromagnetic resonance spin pumping has been reported.[23] In that case, the amplitude of the spin current depends on the relative alignment of yttrium iron garnet (YIG) and Co magnetization. The dependence of spin dissipation on magnetization direction at the normal mental/FM interface has been observed,[24,25] and the magnetization direction dependence of pure spin current in FMs when the polarization direction of the spin current ($\sigma_{\rm s}$) is non-colinear with $M_{\rm FM}$ has attracted much attention.[26,27]

In this paper, we provide a scheme to observe the magnetization-direction-dependent ISHE in FM. In the IrMn/NiFe/Cu/YIG multilayer structure shown in Fig. 1, we used the ferromagnetic insulating YIG thin film as the spin injector, and the ferromagnetic metal NiFe layer as the spin detector. Due to the interfacial exchange anisotropy between NiFe and IrMn, the NiFe shows up unidirectional anisotropy. Since the YIG film is magnetically soft in plane, the magnetization direction of the YIG ($M_{\rm YIG}$) layer can be rotated by a small magnetic field while the magnetization direction of the NiFe ($M_{\rm NiFe}$) layer is fixed. As shown in Figs. 1(a) and 1(b), the $M_{\rm NiFe}$ is parallel and perpendicular to $M_{\rm YIG}$, respectively. Thus the $\sigma_{\rm s}$ of the spin current emitted by the SSE due to the thermal gradient across the YIG layer can be parallel or perpendicular to $M_{\rm NiFe}$. Therefore, the ISHE voltages in the NiFe layer in both cases can be observed. The Cu layer was inserted between the NiFe and YIG layers to clearly decouple the two layers.[15] Since the thickness of the Cu layer is much smaller

*Project supported by the National Basic Research Program of China (Grant No. 2015CB921502), the National Natural Science Foundation of China (Grant Nos. 11474184 and 11627805), the 111 Project, China (Grant No. B13029), and the Fundamental Research Funds of Shandong University, China.

†Corresponding author. E-mail: skang@sdu.edu.cn

© 2019 Chinese Physical Society and IOP Publishing Ltd

than its spin diffusion length and it has very weak spin–orbit coupling, the spin current can pass through the Cu layer in the IrMn/NiFe/Cu/YIG sample with the ISHE voltage induced in the Cu layer negligible.

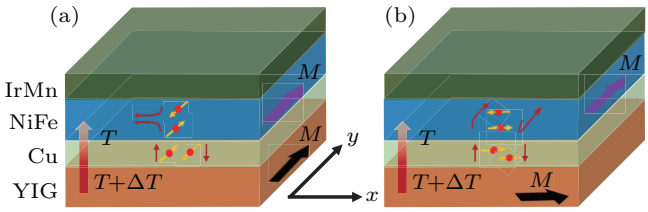


Fig. 1. Schematic setup for measuring the inverse spin Hall effect (ISHE) in NiFe layer induced by longitudinal spin Seebeck. Here, ΔT and M denote the temperature gradient and magnetization directions of ferromagnets, respectively. An exchange bias field is induced in NiFe. The orientations of spin current which is emitted by the longitudinal spin Seebeck are parallel and perpendicular to the magnetization direction of the NiFe layer in panels (a) and (b), respectively.

2. Experimental details

The YIG films of 100 nm were deposited on (111) single crystal substrates of gadolinium gallium garnet (GGG). The YIG/GGG films were annealed at 85 °C in a tube furnace flowing oxygen gas for 2 h. After annealing the YIG film, the IrMn(8)/NiFe(8)/Cu(4) were deposited on YIG, and then 100 nm Au electrodes were also deposited. A a control sample of IrMn(8)/NiFe(8)/Cu(4) on naturally oxidized Si substrate (SiO_2-Si) was also prepared. A 10 nm SiO_2 capping layer was deposited to protect from oxidation for all samples. All films were prepared with a magnetron sputtering system at room temperature, and the base pressure was better than 3×10^{-6} Pa. The IrMn/NiFe/Cu and the Au films were both patterned with shadow masks, whose sizes are shown in Fig 2(b). During deposition of IrMn(8)/NiFe(8)/Cu(4), an in-plane static field of about 400 Oe was applied to induce an easy magnetization axis in the NiFe/IrMn layers. As shown in Fig. 2(a), the morphology of the YIG film, with a root mean square (RMS) roughness of 0.21 nm, tracks the atomically flat terraces. The magnetic hysteresis loop of the YIG film measured by an alternative gradient magnetometer (AGM) with magnetic field swept in the film plane at room temperature is shown in Fig. 2(c). The YIG film is magnetically soft with an in-plane saturation field of about 30 Oe, and its saturation magnetization is determined to be about 1.59 kG ($4\pi M_s$). As shown in Fig. 2(d), the out-of-plane saturation field is roughly equal to the value of $4\pi M_s$.

The longitudinal SSE measurement method is shown in Fig. 2(b). A temperature gradient was applied along the z direction. The DC voltages were measured with Keithley 2182 nanovoltmeters between electrodes a and b (y direction, V_{ab}), and c and d (x direction, V_{cd}) with a rotatable magnetic field applied in the x–y plane. The easy magnetization axis of NiFe was along the $+y$ direction.

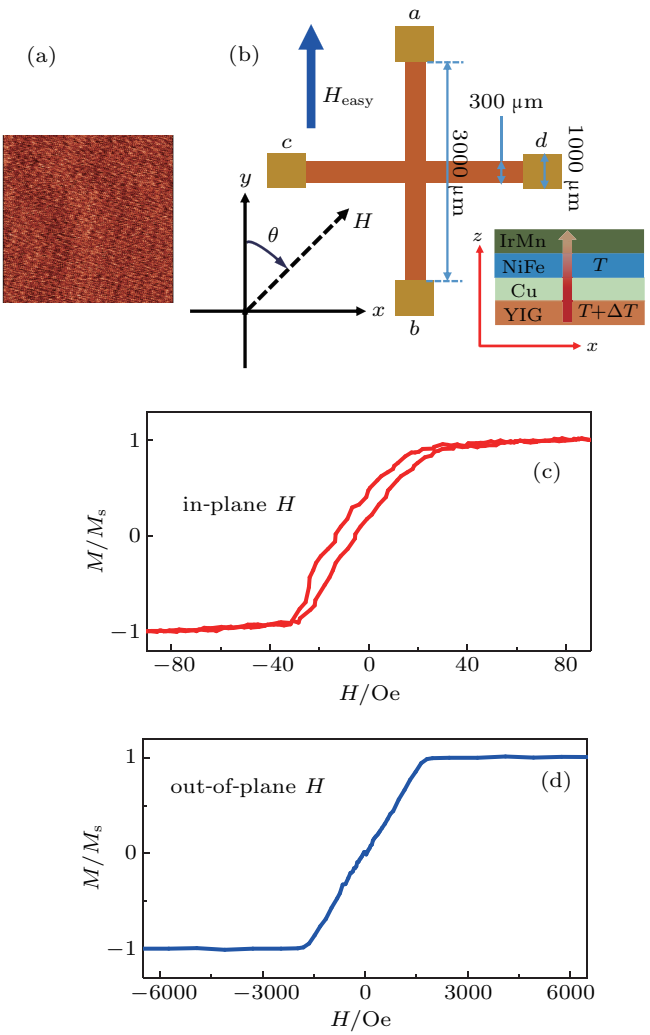


Fig. 2. (a) Atomic force microscopy (AFM) image of 100 nm YIG film on GGG (111). (b) The size of the sample and the measurement method. Here, thermal gradient ΔT is along the z direction, the easy magnetization axis of the NiFe layer is along the $+y$ direction, and the rotatable magnetic field is applied in the x–y plane. (c) The in-plane hysteresis loop of 100 nm YIG. (d) The out-of-plane hysteresis loop of 100 nm YIG.

3. Results and discussion

To compare the amplitudes of SSE voltages for $M_{\rm NiFe}\perp\sigma_{\rm s}$ (V_{ab}) and $\sigma_{\rm s}\parallel M_{\rm NiFe}$ (V_{cd}), $M_{\rm NiFe}$ and $M_{\rm YIG}$ should be fixed and rotatable with a rotatable magnetic field, respectively, during the SSE measurement in the sample of IrMn(8)/NiFe(8)/Cu(4)/YIG(100)/GGG. A small rotatable magnetic field of 35 Oe, which is larger than the saturation field of YIG, was applied to rotate $M_{\rm YIG}$. Before the SSE measurement with a small magnetic field, a large magnetic field of 1000 Oe was first applied along the $+y$ direction (the easy axis of NiFe) to saturate $M_{\rm NiFe}$. After removing the magnetic field of 1000 Oe, the SSE measurement with a rotatable magnetic field of 35 Oe was performed.

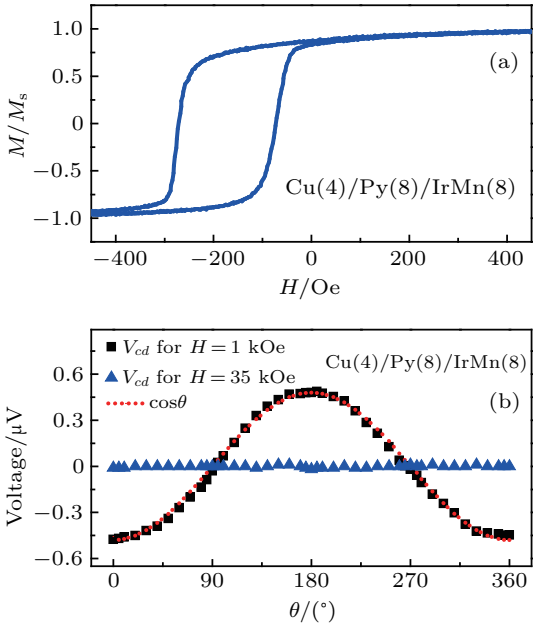


Fig. 3. (a) The in-plane hysteresis loop of IrMn(8)/NiFe(8)/Cu(4)/SiO_2 by a magnetic field sweeping along the easy magnetization axis of NiFe. (b) Magnetization direction dependence of SSE voltages for the sample of IrMn(8)/NiFe(8)/Cu(4)/SiO_2 with rotatable magnetic fields of 35 Oe and 1000 Oe.

The IrMn(8)/NiFe(8)/Cu(4)/YIG(100)/GGG magnetic hysteresis loop with a magnetic field swept along the easy magnetization axis of NiFe is shown in Fig. 4(a). The bias field of about 230 Oe is much larger than the rotatable magnetic field of 35 Oe. To examine whether $M_{\rm NiFe}$ was changed with the small rotatable magnetic field of 35 Oe, the comparison measurement was performed on IrMn(8)/NiFe(8)/Cu(4)/SiO_2. When $M_{\rm NiFe}$ rotated with the applied magnetic field, both anomalous Nernst and spin Seebeck voltages would be induced due to the thermal gradient across the NiFe layer in the IrMn(8)/NiFe(8)/Cu(4)/SiO_2. As shown in Fig. 3(b), compared to that for $H = 1000$ Oe, the voltage for $H = 35$ Oe was negligible, indicating a nearly unchanged $M_{\rm NiFe}$ in IrMn(8)/NiFe(8)/Cu(4)/SiO_2 when a magnetic field of 35 Oe was applied. As shown in Fig. 3(a), the bias field of NiFe in the sample of IrMn(8)/NiFe(8)/Cu(4)/SiO_2 is about 200 Oe, which is a bit smaller than that of NiFe in the sample of IrMn(8)/NiFe(8)/Cu(4)/YIG(100)/GGG. Therefore, $M_{\rm NiFe}$ in the sample of IrMn(8)/NiFe(8)/Cu(4)/YIG(100)/GGG should be nearly unchanged when a small rotatable magnetic field of 35 Oe was applied. The magnetization direction dependence of SSE voltages measured in the sample of IrMn(8)/NiFe(8)/Cu(4)/YIG(100)/GGG with a small rotatable magnetic field of 35 Oe is shown in Fig. 4(b). We can find that the amplitude of V_{cd} is about 30% larger than that of V_{ab}, indicating a larger SSE voltage induced for $\sigma_{\rm s} \parallel M_{\rm NiFe}$ (V_{cd}) than that for $\sigma_{\rm s} \perp M_{\rm NiFe}$ (V_{ab}). When a rotatable magnetic field of 1000 Oe was applied in the sample of IrMn(8)/NiFe(8)/Cu(4)/YIG(100)/GGG, $M_{\rm YIG}$ and $M_{\rm NiFe}$ were both saturated and $\sigma_{\rm s}$ was always parallel to $M_{\rm NiFe}$. As shown in Fig. 4(c), the nearly identical amplitudes of V_{ab} and V_{cd} are observed during the SSE measurement with a rotatable magnetic field of 1000 Oe. We should point out that the value of $(R_{ab} - R_{cd})/(R_{ab} + R_{cd})$ is less than 1.5%, where R_{ab} and R_{cd} are the resistances between electrodes a and b, and c and d, respectively. Therefore the amplitude difference of V_{ab} and V_{cd} (as shown in Fig. 4(b)) cannot result from the non-uniformity of the sample. In addition, the spin current emitted by the SSE in the YIG layer may flow into the IrMn layer after passing through the Cu and NiFe layers. If we assume that the spin diffusion length of NiFe $\lambda_{\rm NiFe} = 2.5$ nm,[28] the spin current flowing into the IrMn layer after passing through the 8 nm NiFe layer will be very weak, thus allowing us to ignore the ISHE voltage induced in the IrMn layer.

In general, the $V_{\rm SSE}$ induced in the sample of IrMn(8)/NiFe(8)/Cu(4)/YIG(100)/GGG can be expressed as[14]

$$V_{\rm SSE} \propto AL\Delta T(\rho_{\rm NiFe}\theta_{\rm SH}^{\rm NiFe})\left(\frac{\lambda_{\rm NiFe}}{t_{\rm NiFe}}\tanh\left(\frac{t_{\rm NiFe}}{2\lambda_{\rm NiFe}}\right)\right), \quad (1)$$

a product of three terms. The first term includes the spin injection coefficient A, the thermal gradient ΔT across the YIG layer, and the sample dimension L. The second term includes the electrical resistivity $\rho_{\rm NiFe}$ and the spin Hall angle $\theta_{\rm SH}^{\rm NiFe}$ of NiFe. The third term describes the decay of pure spin current due to spin diffusion length $\lambda_{\rm NiFe}$ and layer thickness $t_{\rm NiFe}$ of NiFe. We assume that the spin Hall angles of NiFe for $\sigma_{\rm s} \perp M_{\rm NiFe}$ and $\sigma_{\rm s} \parallel M_{\rm NiFe}$ are the same. The scattering strength to spin current at NiFe/Cu interface, which is related to the interfacial spin injection coefficient A, may be different. The value of A for $\sigma_{\rm s} \parallel M_{\rm NiFe}$ may be larger than that for $\sigma_{\rm s} \perp M_{\rm NiFe}$, thus allowing more spin current injection into the NiFe layer for $\sigma_{\rm s} \parallel M_{\rm NiFe}$. This may induce a larger ISHE voltage for $\sigma_{\rm s} \parallel M_{\rm NiFe}$ than that for $\sigma_{\rm s} \perp M_{\rm NiFe}$. Besides, the bulk scattering strength may be different in the two cases, where different spin diffusion lengths in NiFe may be induced. In comparison with that for $\sigma_{\rm s} \parallel M_{\rm NiFe}$, the bulk scattering strength to spin current for $\sigma_{\rm s} \perp M_{\rm NiFe}$ may be stronger, which may induce a shorter spin diffusion length in the NiFe layer. If we assume that $\lambda_{\rm NiFe} = 2.5$ nm[15] for $\sigma_{\rm s} \parallel M_{\rm NiFe}$ and $\lambda_{\rm NiFe} < 2.5$ nm for $\sigma_{\rm s} \perp M_{\rm NiFe}$, the value of the third term of Eq. (1) for $\sigma_{\rm s} \perp M_{\rm NiFe}$ is less than that for $\sigma_{\rm s} \parallel M_{\rm NiFe}$, indicating a samller voltage induced for $\sigma_{\rm s} \perp M_{\rm NiFe}$. In the SMR measurement, the larger spin dissipation for $\sigma_{\rm s} \perp M_{\rm NiFe}$ at the interface of normal mental/FM has been observed.[24,25,29] Therefore, the smaller SSE voltage for $\sigma_{\rm s} \perp M_{\rm NiFe}$ than that for $\sigma_{\rm s} \parallel M_{\rm NiFe}$ may originate from either or both of stronger interface and bulk scatterings for $\sigma_{\rm s} \perp M_{\rm NiFe}$.

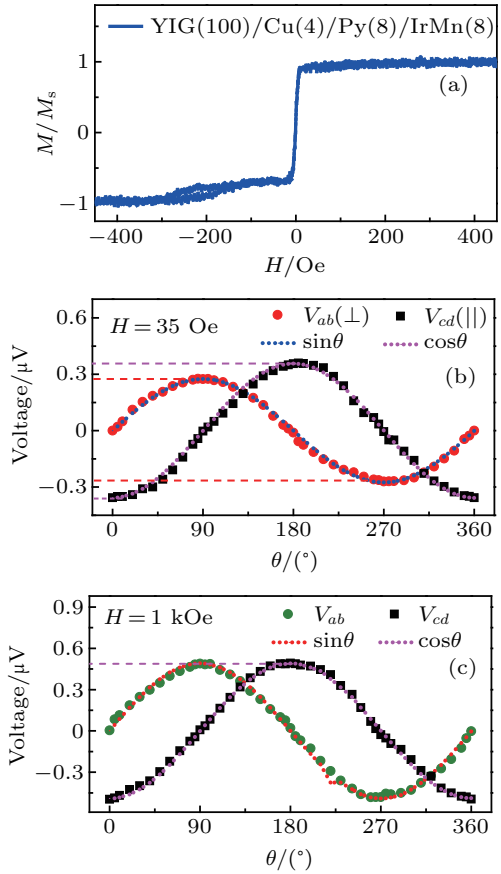


Fig. 4. (a) The IrMn(8)/NiFe(8)/Cu(4)/YIG(100)/GGG in-plane hysteresis loop by sweeping a magnetic field along the easy magnetization axis of NiFe. Panels (b) and (c) show the magnetization direction dependence of the SSE voltages for the sample of IrMn(8)/NiFe(8)/Cu(4)/YIG(100)/GGG with rotatable magnetic fields of 35 Oe and 1000 Oe, respectively.

4. Conclusion

The magnetization-direction-dependent ISHE has been observed in IrMn/NiFe/Cu/YIG multilayer structure. When a small rotatable magnetic field is applied, the magnetization direction of the YIG layer can be rotated, while the magnetization direction of the NiFe layer is fixed by the exchange bias field. By this means, we can regulate the relative orientation of σ_s and M_{NiFe}. The spin Seebeck voltage for $\sigma_s \parallel M_{NiFe}$ is about 30% larger than that for $\sigma_s \perp M_{NiFe}$. This amplitude difference of SSE signals may originate from either or both of stronger interface scattering at Cu/NiFe and bulk scattering in NiFe when $\sigma_s \perp M_{NiFe}$. Our result provides a way to control the ISHE voltage induced in ferromagnets.

References

[1] žutić I, Fabian J and Sarma S D 2004 *Rev. Mod. Phys.* **76** 323

[2] Wolf S A, Awschalom D D, Buhrman R A, Daughton J M, Molna S V, Roukes M L, Chtchelkanova A Y and Treger D M 2001 *Science* **294** 1488

[3] Ando K, Kajiwara Y, Takahashi S, Maekawa S, Takemoto K, Takatsu M and Saitoh E 2008 *Phys. Rev. B* **78** 014413

[4] Saitoh E, Ueda M, Miyajima H and Tatara G 2006 *Appl. Phys. Lett.* **88** 182509

[5] Mosendz O, Pearson J E, Fradin F Y, Bauer G E W, Bader S D and Hoffmann A 2010 *Phys. Rev. Lett.* **104** 046601

[6] Kang Y, Zhong H, Hao R R, Hu S J, Kang S S, Liu G L, Zhang Y, Wang X R, Yan S S, Wu Y, Yu S Y, Han G B Jiang Y and Mei L M 2017 *Chin. Phys. B* **26** 047202

[7] Hirsch J E 1999 *Phy. Rev. Lett.* **83** 1834

[8] Uchida K, Takahashi S, Harii K, Ieda J, Koshibae W, Ando K, Maekawa S and Saitoh E 2008 *Nature* **455** 778

[9] Kikkawa T, Uchida T, Shiomi Y, Qiu Z, Hou D, Tian D, Nakayama H, Jin X F and Saitoh E 2013 *Phys. Rev. Lett.* **110** 067207

[10] Huang S Y, Wang W G, Lee S F, Kwo J and Chien C L 2011 *Phys. Rev. Lett.* **107** 216604

[11] Kimura T, Otani Y, Sato T, Takahashi S and Maekawa S 2007 *Phys. Rev. Lett.* **98** 156601

[12] Wang H L, Du C H, Pu Y, Adur R, Hammel P C and Yang F Y 2014 *Phys. Rev. Lett.* **112** 197201

[13] Du C, Wang H, Yang F and Hammel P C 2014 *Phys. Rev. B* **90** 140407

[14] Tian D, Li Y F, Qu D, Jin X F and Chien C L 2015 *Appl. Phys. Lett.* **106** 212407

[15] Miao B F, Huang S F, Qu D and Chien C L 2013 *Phys. Rev. Lett.* **111** 066602

[16] Wu H, Wan C H, Yuan Z H, Zhang X, Jiang J, Zhang Q T, Wen Z C and Han X F 2015 *Phys. Rev. B* **92** 054404

[17] Hao R R, Zhong H, Kang Y, Tian Y F, Yan S S, Liu G L, Han G B, Yu S Y, Mei L M and Kang S S 2018 *Chin. Phys. B* **27** 037202

[18] Wu H, Wang X, Huang L, Qin J Y, Fang C, Zhang X, Wan C H and Han X F 2017 *J. Magn. Magn. Mater.* **441** 149

[19] Djayaprawira D D, Tsunekawa K, Nagai M, Maehara H, Yamagata S, Watanabe N, Yuasa S, Suzuki Y and Ando K 2005 *Appl. Phys. Lett.* **86** 092502

[20] Binasch G, Grünberg P, Saurenbach F and Zinn W 1989 *Phys. Rev. B* **39** 4828

[21] Baibich M N, Broto J M, Fert A, Nguyen V D F, Petroff F, Etienne P, Creuzet G, Friederich A and Chazelas J 1988 *Phys. Rev. Lett.* **61** 2472

[22] Miyazaki T and Tezuka N 1995 *J. Magn. Magn. Mater.* **139** L231

[23] Cramer J, Fuhrmann F, Ritzmann U, Gall V, Niizeki T, Ramos R, Qiu Z, Hou D, Kikkawa T, Sinova J, Nowak U, Saitoh E and Klaui M 2018 *Nat. Commun.* **9** 1089

[24] Chen Y T, Takahashi S, Nakayama H, Althammer M, Goennenwein S T B, Saitoh E and Bauer G E W 2013 *Phys. Rev. B* **87** 144411

[25] Althammer M, Meyer S, Nakayama H, Schreier M, Altmannshofer S, Weiler M, Huebl H, Geprägs S, Opel M, Gross R, Meier D, Klewe C, Kuschel T, Schmalhorst J M, Reiss G, Shen L, Gupta A, Chen Y T, Bauer G E W, Saitoh E and Goennenwein S T B 2013 *Phys. Rev. B* **87** 224401

[26] Das K S, Schoemaker W Y, van Wees B J and Vera-Marun I J 2017 *Phys. Rev. B* **96** 220408

[27] Qin C, Chen S H, Cai Y J, Kandaz F and Ji Y 2017 *Phys. Rev. B* **96** 134418

[28] Lu Y M, Choi Y, Ortega C M, Cheng X M, Cai J W, Huang S Y, Sun L and Chien C L 2013 *Phys. Rev. Lett.* **110** 147207

[29] Marmion S R, Ali M, McLaren M, Williams D A and Hickey B J 2014 *Phys. Rev. B* **89** 220404